Acta Acustica 2026, **10**, 61
© The Author(s), Published by EDP Sciences, 2026
https://doi.org/10.1051/aacus/2026058

Available online at:
https://acta-acustica.edpsciences.org

Topical Issue - Proceedings of AFPAC 2026

SCIENTIFIC ARTICLE OPEN ACCESS

From the simulation of guided wave propagation in rolled plates subjected to stress to the tomographic reconstruction of stress distributions

Flavien Agon, Alain Lhémery*, and Jordan Barras

Université Paris-Saclay, CEA, List, F-91120 Palaiseau, France

Received 8 April 2026, Accepted 12 June 2026

Abstract – A model capable of predicting guided wave (GW) modes in plates subjected to multiaxial stresses has been developed, initially based on the assumption of an isotropic initial state of the plate. Using tomographic inversion based on a simplified model of these variations, the stresses were successfully mapped. Here, the model is extended to handle the case of a plate that is initially anisotropic due to rolling. First, a simple description of the initial anisotropy is defined. Next, a SAFE-type calculation is used to predict GW in a rolled plate subjected to stresses. Its predictions are compared with results computed by a finite element code for validation purposes. The model is used to conduct parametric studies. More specifically, we investigate the variations in velocity between waves propagating in a stressed and rolled plate and those propagating in an unstressed one, as a function of the direction of propagation and frequency. These variations are then fitted by simple analytical functions that can be inverted and used as a basis for the tomographic reconstruction of stress distributions within a plate. The initial elastic anisotropy due to strong rolling leads to caustics for the SH0 modes that prevent the use of certain range of propagation directions in the tomographic inversion, whilst the velocity variations of qS_0 and qA_0 modes can be successfully used (as in the isotropic case) to map non-uniform stress distributions.

Keywords. Acoustoelasticity, Guided waves, Rolling, Residual stress, GW tomography

1 Introduction

Metal sheets produced in the steel and aluminium industry undergo rolling process, in which their microstructure can be significantly changed, leading to a certain anisotropy. In addition, residual stresses may also be induced. If they reach significant values, these latter can cause problems, notably when cutting the sheet metal during the industrial process of its use. It would be useful to characterize residual stresses and to map them non-destructively to enable a safer use of rolled sheets. But stress characterization methods presently applied industrially are generally local and mostly destructive.

In a previous study, we developed a guided wave (GW) tomography method [1] for determining multiaxial residual stress maps. This tomography method was based on a simple invertible model describing the variations in velocity of the different guided modes resulting from stresses, relative to propagation in a stress-free reference state. These variations are integrated along all wave paths between each pair of transmitters and receivers involved in the tomographic reconstruction. The model itself was developed from results obtained using a theoretical model of acoustoelastic (AE) effects on guided waves [2]. It should be noted that a recent review about AE on GW has been published [3], to which interested readers are referred. In this review, several other contributions published after ours [2] but of a similar nature are described for modelling these effects.

In our previous works, both the tomographic inversion and the theoretical forward model assumed that the stress-free sheet, in its natural state, was elastically isotropic. The objective of the present study is twofold: (i) we want to extend the capabilities of the theoretical model to the case where the metal sheet is initially anisotropic, in order to (ii) determine whether findings made previously in the case of stress-free isotropic sheets can be adapted to the case of sheets that are initially anisotropic due to rolling.

The paper is organized as follows. The second section describes different tools to attain our goals. A simple tool for describing anisotropy due to rolling is first presented

*Corresponding author: alain.lhemery@cea.fr

that is based on a single parameter to account for varying rolling force that can be easily varied for parametric studies. Then, the extension of the model derived in our previous work [2] is described. It takes into account the combined effects of stress and rolling. It is specifically applied to the computation of GW modes. Computed GW modes are introduced in a field radiation model [4] to compare predictions of the new model with those computed with a finite element code [5] dealing with waves in stressed media for validation. In the third section, a parametric study is carried out with the proposed model to determine whether and how the previous conclusions concerning the feasibility of tomographic inversion for mapping multiaxial residual stresses in a plate when the reference stress-free state is isotropic also apply to rolled sheets. Simple invertible formulas readily usable in tomographic inversion are obtained for the velocity variations due to stress in a rolled plate relatively to the unstressed rolled plate (for Lamb waves and with restrictions for shear horizontal mode) similar to formulas previously obtained in the isotropic case [1].

2 Theory of GW propagation in stressed, rolled plate

This section aims to present a model for predicting a modal solution for guided wave propagation in a plate that is initially rolled and that undergoes stress. Residual or applied stresses and rolling cause anisotropy, and these phenomena combine. In order to adapt the guided wave tomography method proposed for an initially isotropic plate to the case of a rolled plate, it is essential to be able to deal with these phenomena and their combination. First, simple formulae are presented (Sect. 2.1) that are derived from a classical model for generating various states of anisotropic elasticity of a medium structured by rolling. These states are easily varied by means of a single parameter, easing further parametric studies. Next (Sect. 2.2), the model combining acousto-elasticity to deal with effect of stress on the initially anisotropic medium is described and applied to GW modal computations. Elements of validation are shown in Section 2.3 by means of comparison of results computed by the present model with results predicted by a very different method (time-dependent finite element method).

2.1 Simple description of anisotropy induced by rolling

Here, we present a simple method for describing the elastic anisotropy of a sheet textured by rolling. The effects of rolling on microstructures have been the subject of numerous studies over the past few decades. Interested readers are referred to a recent review [6] on this subject: various models can be used to predict the effects of the many parameters that influence the microstructure resulting from phenomena occurring during rolling processes (of steel sheets in this study). Our aim here is

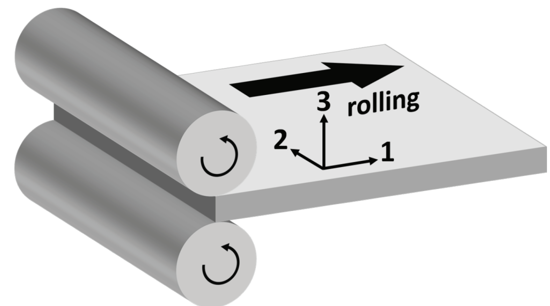

Figure 1. Schematic diagram of the rolling process in which the plate moves relative to axis 1.

to provide a simple description of the global anisotropic elastic state (second-order elastic constants) of a sheet resulting from a rolling process, as well as a realistic range of variation for this state.

In many publications about the effects of texturing on elastic constants, a polycrystalline medium is considered made of cubic monocrystal of constants C^0_{11}, C^0_{12}, C^0_{44}. The Voigt procedure, which consists of calculating the average of the elastic constants of a polycrystal is followed: the preferred orientation of crystallites is described by the orientation distribution coefficients W_{lmn} (ODC). Assuming orthorhombic symmetry and considering the axes defined as shown in Figure 1, axis 1 being the direction of advancement of the plate in the rolling process, the nine independent orthorhombic constants are expressed as functions of only three ODCs W_{400}, W_{420} and W_{440}.

Defining $C^0 \equiv C^0_{11} - C^0_{12} - 2C^0_{44}$, the orthorhombic constants are classically expressed by (see [7] for example)

$$C_{11} = C^0_{11} - 2C^0\left(\frac{1}{5} - \frac{6}{35}\sqrt{2}\pi^2 \times \left[W_{400} - \frac{2}{3}\sqrt{10}W_{420} + \frac{1}{3}\sqrt{70}W_{440}\right]\right), \quad (1a)$$

$$C_{22} = C^0_{11} - 2C^0\left(\frac{1}{5} - \frac{6}{35}\sqrt{2}\pi^2 \times \left[W_{400} + \frac{2}{3}\sqrt{10}W_{420} + \frac{1}{3}\sqrt{70}W_{440}\right]\right), \quad (1b)$$

$$C_{33} = C^0_{11} - 2C^0\left(\frac{1}{5} - \frac{16}{35}\sqrt{2}\pi^2 W_{400}\right), \quad (1c)$$

$$C_{44} = C^0_{44} + C^0\left(\frac{1}{5} - \frac{16}{35}\sqrt{2}\pi^2\left[W_{400} + \sqrt{\frac{5}{2}}W_{420}\right]\right), \quad (1d)$$

$$C_{55} = C^0_{44} + C^0\left(\frac{1}{5} - \frac{16}{35}\sqrt{2}\pi^2\left[W_{400} - \sqrt{\frac{5}{2}}W_{420}\right]\right), \quad (1e)$$

$$C_{66} = C^0_{44} + C^0\left(\frac{1}{5} + \frac{4}{35}\sqrt{2}\pi^2\left[W_{400} - \sqrt{70}W_{440}\right]\right), \quad (1f)$$

$$C_{23} = C_{12}^0 + C^0\left(\frac{1}{5} - \frac{16}{35}\sqrt{2}\pi^2\left[W_{400} + \sqrt{\frac{5}{2}}W_{420}\right]\right), \tag{1g}$$

$$C_{31} = C_{12}^0 + C^0\left(\frac{1}{5} - \frac{16}{35}\sqrt{2}\pi^2\left[W_{400} - \sqrt{\frac{5}{2}}W_{420}\right]\right), \tag{1h}$$

$$C_{12} = C_{12}^0 + C^0\left(\frac{1}{5} + \frac{4}{35}\sqrt{2}\pi^2\left[W_{400} - \sqrt{70}W_{440}\right]\right). \tag{1i}$$

These expressions are fairly simple and methods for inverting them and determining the three ODCs from measured ultrasonic wave velocities have been extensively studied.

Assuming for simplicity that the effects of rolling leading to thinning of the metal sheet exhibit higher symmetry, namely, transverse isotropy, only five independent constants fully define the homogeneous medium at the macroscale. Under this assumption, four relations between C_{ij} are taken into account

$$C_{12} = C_{13}, \tag{2a}$$
$$C_{22} = C_{33}, \tag{2b}$$
$$C_{55} = C_{66}, \tag{2c}$$
$$C_{44} = \frac{C_{22} - C_{23}}{2}. \tag{2d}$$

Introducing equations (2) into equations (1) and after some algebra, two simple relations between the three ODCs involved are obrained

$$W_{440} = \frac{\sqrt{70}}{6}W_{400}, \tag{3a}$$
$$W_{420} = \frac{\sqrt{10}}{3}W_{400}. \tag{3b}$$

Finally, substituting equations (3) into equations (1) allows us to express the elastic constants of the transversely isotropic medium constituting the laminated plate. We get

$$C_{11} = C_{11}^0 - 2C^0\left(\frac{1}{5} - \frac{128}{105}\sqrt{2}\pi^2 W_{400}\right), \tag{4a}$$
$$C_{22} = C_{33} = C_{11}^0 - 2C^0\left(\frac{1}{5} - \frac{16}{35}\sqrt{2}\pi^2 W_{400}\right), \tag{4b}$$
$$C_{12} = C_{13} = C_{12}^0 + C^0\left(\frac{1}{5} - \frac{128}{105}\sqrt{2}\pi^2 W_{400}\right), \tag{4c}$$
$$C_{23} = C_{12}^0 + C^0\left(\frac{1}{5} + \frac{32}{105}\sqrt{2}\pi^2 W_{400}\right), \tag{4d}$$
$$C_{55} = C_{66} = C_{44}^0 + C^0\left(\frac{1}{5} - \frac{128}{105}\sqrt{2}\pi^2 W_{400}\right), \tag{4e}$$
$$C_{44} = C_{44}^0 + C^0\left(\frac{1}{5} + \frac{32}{105}\sqrt{2}\pi^2 W_{400}\right). \tag{4f}$$

Table 1. Numerical values of cubic crystals C_{ij}^0 [in GPa] and C^0 taken for further computation, based on steel properties in [8].

C_{11}^0 (GPa)	C_{12}^0 (GPa)	C_{44}^0 (GPa)	C^0 (GPa)
237	141	116	−136

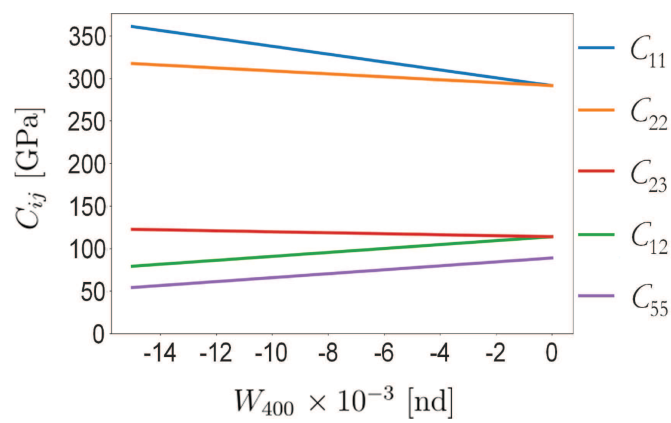

Figure 2. Variations of the five stiffness constants defining different transversely isotropic materials as functions of the ODC W_{400}.

The sixth equation is redundant, as the first five fully define the transverse isotropy. Anisotropy at the macroscale is therefore described either by five independent constants C_{11}, C_{22}, C_{12}, C_{23} and C_{55} or by the three constants C_{11}^0, C_{12}^0, C_{44}^0 of the cubic single crystal and one ODC, W_{400}. In Hirao and Ogi's book [7], a chapter, which includes many references to previous and foundational works on elasticity of textured materials, is devoted to texture monitoring. Equations (1) given above are described exhaustively and the decreasing linear relationship between W_{400} and the average plastic strain ratio $\bar{r}$ is examined. This ratio $\bar{r}$ can be related to rolling parameters. The values of the elastic constants C_{ij}^0 of the cubic crystal as well as the value of C^0 taken into account in what follows for the material considered (steel) are given in Table 1.

We can now examine the (linear) variations of the five independent coefficients C_{ij} as a function of W_{400}, as shown in Figure 2. These values converge to three distinct constants as W_{400} approaches zero, which corresponds to elastic isotropy. Indeed, one of these three constants depends on the other two.

Now, as an example of typical anisotropy induced by rolling in a plate, we consider a 3-mm-thick steel plate subjected to rolling associated with different values of W_{400} (low, mid and high). Figure 3 displays the energy velocity of the three fundamental guided modes (below the first cut-off frequency) by angular plots. Because of symmetries, it is enough to display them in a quadrant from 0° (along the axis 1 of rolling) to 90° (axis 2). Modes are computed using our implementation of the semi-analytical finite element (SAFE) method [4] for anisotropic plates.

For high rolling, leading to highest anisotropy, caustics (inflection points of the velocity curve) appear in Figure 3c for the SH_0 mode. Within a small angular range between these caustics, in a given direction of energy, up to three wavefronts appear. This is important to study because the use of time-of-flight between emitters and receivers to measure wave velocity variations is the basis of the tomographic method we want to develop. Figure 4 shows how the angular range between two caustics for the SH_0 mode varies with W_{400}. They appear for absolute values of W_{400} higher than 4.5×10^{-3}. This has been computed at two different frequencies. The angular range does not depend on frequency, and is roughly linearly dependent on W_{400}. As soon as rolling leads to these values of W_{400}, it is not possible to determine a single energy velocity for SH_0 waves within this angular range, which must be excluded from any tomographic inversion process. As a consequence, for strong rolling force, only the two fundamental Lamb modes can be used safely for inversion.

The present simple description is not a necessary step for achieving our overall goal of stress characterization. There exist many methods to obtain the five independent elastic constants describing at a macroscale a transversely isotropic medium. Here, it is only a simple way of synthesizing various anisotropic unstressed media by considering various values of a single parameter to ease simulation studies.

2.2 Simple model of acoustoelastic effects in anisotropic plates

Modelling waves whose propagation is affected by acoustoelastic phenomena in a stressed medium is far more complex than modelling waves propagating in an elastic medium. In the most general case (with the weakest symmetries), 21 second-order independent elastic constants (SOECs) are involved in linear elasticity theory, whereas 21 SOECs plus 56 third-order independent constants (TOECs) are involved in acoustoelastic theory. This simple fact clearly shows that it is not feasible in practice to develop a method for characterising stresses based on the inversion of measurements using algorithms relying on a precise theoretical description of wave propagation in these most general media. It is therefore necessary to formulate simplifying assumptions regarding the symmetries of these phenomena, to model them using a limited number of independent constants that can be measured in practice.

Th simple description in the previous paragraph is an example of such a simplification where the unstressed but rolled plate, taken to be the natural state [2] is considered to be made of a homogeneous transversally isotropic medium. Here, we follow a similar approach to model phenomena associated with acoustoelasticity.

The idea consists mostly in re-using the previous theoretical work derived in [2], which resulted in the developments of a semi-analytical finite element (SAFE) method to predict the GW modes propagating in an isotropic plate submitted to multi-axial stresses. The overall theory and its use for the development of GW solutions computed by the acoustoelastic SAFE method (AE-SAFE in what follows) are presented in details in this reference and adopted here. The main formulae given in [2] and the computer model implementing them are the bases of the present work.

The assumptions made here consist in considering that (i) the unstressed medium (taken to be the natural state) is transversally isotropic with an axis of symmetry along the rolling direction 1, requiring the knowledge of five independent SOEC; (ii) locally, acoustoelastic effects are described similarly as those that would take place in an isotropic plate and are only dependent on the local direction of stress relatively to the propagation direction of the GW. Therefore, as far as TOEC are concerned, only three independent constants, the Murnaghan constants l, m, n are required.

Finally, the only difference to combine acoustoelasticity and anisotropy of the natural state is to replace the simple expressions of the SOEC as functions of Lamé coefficient by the actual values of the constants obtained in the previous subsection. The various TOEC are otherwise expressed as functions of the Murnaghan constants l, m, n as

$$\begin{aligned} C_{ijklmn} &= 2\left(l - m + \frac{n}{2}\right)\delta_{ij}\delta_{kl}\delta_{mn} \\ &+ 2\left(m - \frac{n}{2}\right)\left(\delta_{ij}I_{klmn} + \delta_{kl}I_{mnij} + \delta_{mn}I_{ijkl}\right) \\ &+ \frac{n}{2}\left(\delta_{ik}I_{jlmn} + \delta_{il}I_{jkmn} + \delta_{jk}I_{ilmn} + \delta_{jl}I_{ikmn}\right), \end{aligned} \tag{5a}$$

$$I_{ijkl} = \frac{\delta_{ik}\delta_{jl} + \delta_{il}\delta_{jk}}{2}. \tag{5b}$$

Standard developments of the SAFEM dealing with linear elastodynamics use the symmetries of C_{ijkl}. Voigt notation is used to transform the 4th order stiffness tensor into a 6×6 matrix of SOEC. Here, the equivalent stiffness tensor $\mathbf{C}^{eq}$ resulting from acoustoelasticity does not possess these symmetries (as explained in [2]). To apply the SAFE method in the presence of stress by accounting for these lower symmetries, a 9×9 matrix can be defined. The following notation is used ($11 \to 1$, $22 \to 2$, $33 \to 3$, $23 \to 4$, $31 \to 5$, $12 \to 6$, $32 \to 7$, $13 \to 8$, $21 \to 9$), allowing to rewrite $\mathbf{C}^{eq}$ (a sixth-order tensor) as a 9×9 matrix. In what follows, we show various 9×9 matrices corresponding to different cases of interest for the present study. The Murnaghan coefficients taken for steel in what follows are given by Table 2.

For the unrolled unstressed plate, the 9×9 matrix $\mathbf{C}^{eq}$ is easily obtained from the usual 6×6 C_{ij} matrix of an isotropic medium. All the symmetries are obvious and the AE-SAFE formulation exactly reduces to the usual

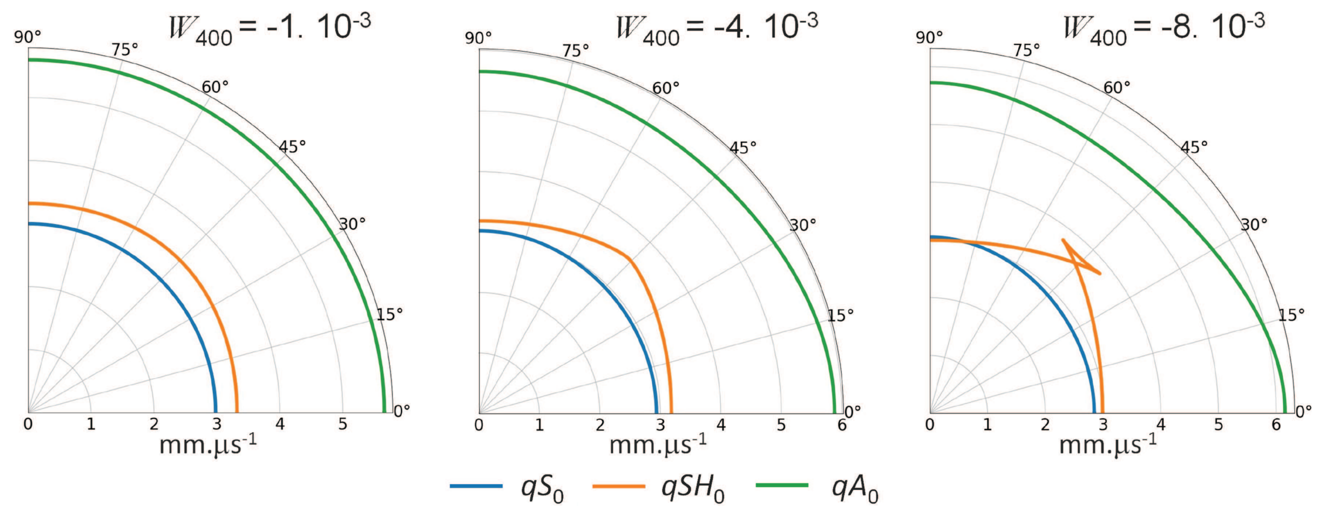

Figure 3. Energy velocities of the three fundamental guided modes at a frequency of 100 kHz for three values of W_{400} [(a) low, (b) medium, (c) high], shown in the range [0°, 90°], 0° being the direction of rolling.

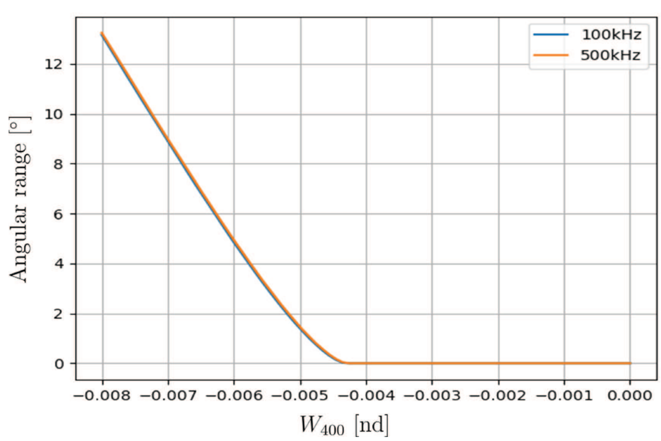

Figure 4. Angular range, in which more than one wavefront of SH_0 mode exist, corresponding to the range between the two caustics, as a function of W_{400}, for two frequencies (100 or 500 kHz).

SAFE formulation for guided modes in isotropic plates. The matrix is given by

$$\begin{pmatrix}
291.4 & 113.8 & 113.8 & & & & & & \\
113.8 & 291.4 & 113.8 & & & & & & \\
113.8 & 291.4 & 291.4 & & & & & & \\
 & & & 88.8 & & & 88.8 & & \\
 & & & & 88.8 & & & 88.8 & \\
 & & & & & 88.8 & & & 88.8 \\
 & & & 88.8 & & & 88.8 & & \\
 & & & & 88.8 & & & 88.8 & \\
 & & & & & 88.8 & & & 88.8
\end{pmatrix}$$

Similarly, for the rolled (along axis 1, with $W_{400} = -4 \times 10^{-3}$) unstressed plate, the 9×9 matrix $\mathbf{C}^{eq}$ is easily obtained from the usual 6×6 C_{ij} matrix of a transversely isotropic plate. Again, the AE-SAFE formulation is equivalent to the usual SAFE formulation for guided modes in transversely isotropic plates. The matrix is now written as:

$$\begin{pmatrix}
309.9 & 104.5 & 104.5 & & & & & & \\
104.5 & 298.3 & 116.1 & & & & & & \\
104.5 & 116.1 & 298.3 & & & & & & \\
 & & & 91.1 & & & 91.1 & & \\
 & & & & 79.5 & & & 79.5 & \\
 & & & & & 79.5 & & & 79.5 \\
 & & & 91.1 & & & 79.5 & & \\
 & & & & 79.5 & & & 79.5 & \\
 & & & & & 79.5 & & & 79.5
\end{pmatrix}$$

Now, for an initially isotropic (unrolled) plate subjected to an axial stress along the axis 1 ($\sigma_1 = 500$ MPa), the acousto-elastic effect results in the creation of an anisotropy with a symmetry, slightly lower than that resulting from rolling as modelled in this paper, as it appears in the 9×9 matrix $\mathbf{C}^{eq}$ given by

$$\begin{pmatrix}
285.9 & 113.2 & 113.2 & & & & & & \\
113.2 & 295.0 & 115.7 & & & & & & \\
113.2 & 115.7 & 295.0 & & & & & & \\
 & & & 89.5 & & & 89.8 & & \\
 & & & & 89.9 & & & 88.6 & \\
 & & & & & 88.3 & & & 88.6 \\
 & & & 89.8 & & & 89.5 & & \\
 & & & & 88.6 & & & 88.3 & \\
 & & & & & 88.6 & & & 88.9
\end{pmatrix}$$

Similarly, for the same initially isotropic (unrolled) plate subjected to an axial stress but this time along the axis 2 ($\sigma_2 = 500$ MPa), the 9×9 matrix $\mathbf{C}^{eq}$ is easily obtained from the previous one by a simple rotation. The values of $\mathbf{C}^{eq}$ (after rotation) are identical. It is given by

Table 2. Murnaghan coefficients for the steel considered in the computations of the present paper.

l (GPa)	m (GPa)	n (GPa)
−750	−999	−1050

$$\begin{pmatrix} 295.0 & 113.2 & 115.7 & & & & & & \\ 113.2 & 285.9 & 113.2 & & & & & & \\ 115.7 & 113.2 & 295.0 & & & & & & \\ & & & 88.3 & & & 88.6 & & \\ & & & & 89.9 & & & 89.8 & \\ & & & & & 88.9 & & & 88.6 \\ & & & 88.6 & & & 88.9 & & \\ & & & & 89.9 & & & 89.5 & \\ & & & & & 88.6 & & & 88.3 \end{pmatrix}$$

Now, for the rolled (along axis 1) and stressed (along the same axis $\sigma_1 = 500\,\mathrm{MPa}$) plate, the symmetries combine easily and the overall symmetry of $\mathbf{C}^{eq}$ is similar to that observed for the unrolled but stressed (along axis 1) case, but with different values due to the natural anisotropy. We get

$$\begin{pmatrix} 304.7 & 104.0 & 104.0 & & & & & & \\ 104.0 & 301.9 & 118.0 & & & & & & \\ 104.0 & 118.0 & 301.9 & & & & & & \\ & & & 91.8 & & & 92.1 & & \\ & & & & 79.7 & & & 79.3 & \\ & & & & & 79.0 & & & 79.3 \\ & & & 92.1 & & & 91.8 & & \\ & & & & 79.3 & & & 79.0 & \\ & & & & & 79.3 & & & 79.7 \end{pmatrix}$$

Eventually, the 9×9 matrix $\mathbf{C}^{eq}$ for the rolled (along axis 1) and stressed (along the axis 2 $\sigma_2 = 500\,\mathrm{MPa}$) plate does not exhibit anymore the same symmetry as before, as expected. In that case, we get

$$\begin{pmatrix} 313.4 & 104.0 & 106.5 & & & & & & \\ 104.0 & 293.0 & 115.6 & & & & & & \\ 106.5 & 115.6 & 301.9 & & & & & & \\ & & & 90.7 & & & 90.9 & & \\ & & & & 80.3 & & & 80.6 & \\ & & & & & 79.7 & & & 79.3 \\ & & & 90.9 & & & 91.3 & & \\ & & & & 80.6 & & & 80.3 & \\ & & & & & 79.3 & & & 79.0 \end{pmatrix}$$

Before using the developed model to conduct a parametric study, we will first provide in the next subsection some elements to demonstrate its validity.

2.3 Elements of validation

In this sub-section, our aim is to give elements of validation of the modal GW solution described in the previous subsection for a stressed and rolled plate. In another work, we developed a modal GW field radiation model [4] accounting for transducer diffraction effects. It is based upon the use of GW modal solutions, which can be computed by whatever means and an approximate theory (pencil method) to predict Green's dyadic linking a point source of surface stress to the particle displacement at an observation point. A simple numerical integration over the sources allows the prediction of the radiated field. This model can use a GW modal solution provided by our AE-SAFE model of GW in rolled and stressed plate. These solutions being obtained for a harmonic excitation, predicting time-dependent field is made possible by Fourier synthesis of these solutions over the source bandwidth.

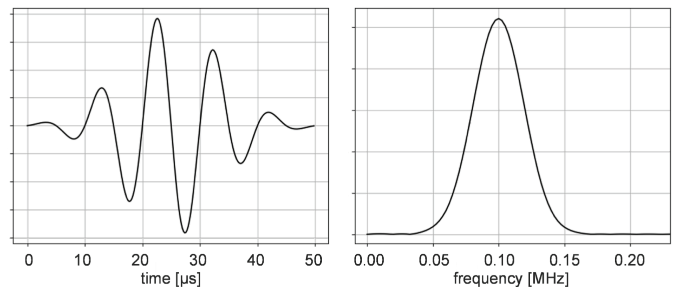

Figure 5. Time-dependency and associated spectrum of the excitation centred on 0.1 MHz used in the validations.

In parallel with the developments described herein, a time-domain finite element method has recently been developed by co-workers [5] to take into account an arbitrary hyperelastic potential in an elastodynamic computation. It can consider various sources of waves. Here, it is used to validate the present model by comparing the predicted waveforms computed by both methods.

The two computational approaches, the modal GW radiation approximate model using modes computed by the AE-SAFE method followed by Fourier synthesis in the one hand, the time-domain FE solution accounting for hyperelastic potential in the other hand, imply very different computations by essence. Comparing their predictions based upon exactly the same input data (material SOEC and TOEC, plate thickness, transducer size, behaviour and excitation) constitutes an efficient way of validation. A few results are given here (among many that are not shown herein for conciseness). A similar approach was used by two of the present authors to validate the modal GW radiation model for an unstressed anisotropic plate [4]. Note that an experimental validation is in preparation for a plate that has been characterized in its nominal state to which controlled stress has been applied.

Here, a 10-mm-diam circular source of normal stress is considered excited by a signal shown on Figure 5. On Figure 6, the u_1 component of the particle displacement predicted at two different points at the surface of the plate, in direction 1 ($\theta = 0°$) and in direction 2 ($\theta = 90°$) 350 mm away from the source centre is shown. Results predicted by both methods are superimposed,

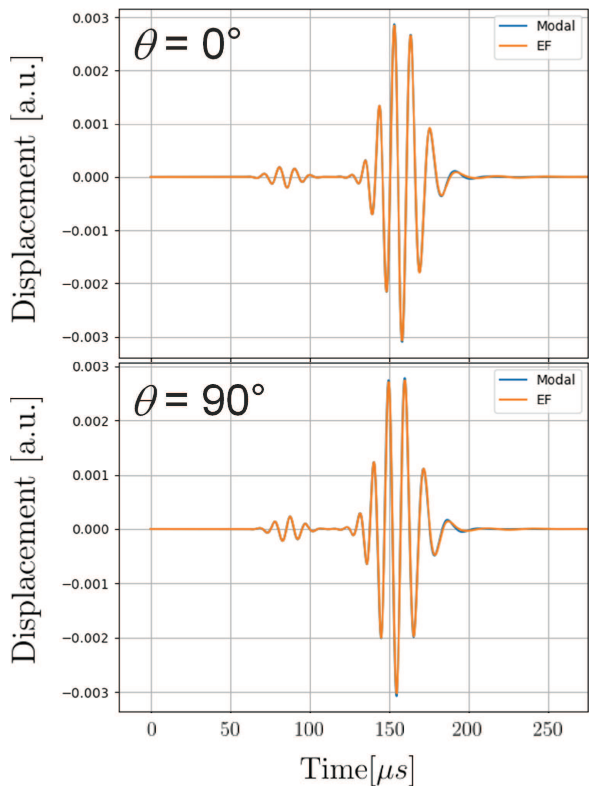

Figure 6. Time-dependent u_1 component of the particle displacement computed by both methods of prediction are shown at two points at the top surface of the rolled plate ($W_{400} = -4.0 \times 10^{-3}$) subjected to an uniform axial stress of 500 MPa along 1. Top: point 350 mm away from the centre of the source along the axis 1. Bottom: same as top, but along the axis 2. Results predicted by the model described in this paper perfectly superimpose with those predicted by the FE method as the time-traces are not discernible.

without scaling. In both cases, waveforms predicted by the two methods superimpose, so much so that it is almost impossible to see there are actually two results for each time-trace shown. The first arriving contribution (around 80 µs) corresponds to the arrival of the qS_0 mode and the second (around 150 µs) corresponds to the arrival of the qA_0 mode. For this excitation, it appears that the qA_0 mode is more dispersive than the qS_0 one. Similar perfect superimpositions were observed for various values of the parameters W_{400}, various values and direction of applied stress and various components of the displacement field.

3 Results

Now that we have a validated simplified model to predict GW modes in a rolled and stressed plate, we can study in details the differences in their behaviour as compared to what was studied before when the natural unstressed state of the plate was modelled as an isotropic medium [1, 2]. As the final goal is the development of a GW tomographic method to reconstruct maps of stresses based onto the inversion of measured time-of-flights variations associated with energy velocity variations along different wavepaths [1], the quantity of interest is the variation, in all possible directions of propagation, of energy velocities of the various modes due to stress relative to those in the unstressed plate. The idea is also to investigate whether, for an initially anisotropic plate, we can draw conclusions similar to those we reached in the case of an initially isotropic plate.

3.1 Parametric studies at one given frequency

In this subsection, the analysis focuses on a specific frequency of 100 kHz. Group velocity variations (percentage) are examined under three distinct scenarios. The first illustrated by Figure 7 shows the influence of texture. It presents the velocity variation of the fundamental modes in a textured medium ($W_{400} = -4.0 \times 10^{-3}$) relative to an isotropic medium, as a function of the energy direction. The second case (Fig. 8) highlights the effect of stress. It describes the velocity variation induced by the acoustoelastic effect due to a given load ($\sigma_1 = 500$ MPa), again relative to an isotropic state. In the case considered of a steel plate, anisotropy due to rolling leads to higher variations than that due to stress. The results obtained for similar calculations but involving an aluminium plate (not presented in this article) show that these two types of induced anisotropy are quantitatively more comparable: texturing results in lower anisotropy, whereas stress results in higher anisotropy. Finally, the last case (Fig. 9) evaluates this same stress-induced variation, but within a textured medium. The specific effect of stress is isolated by subtracting the influence of the texture. It can be seen that the variations in group velocity are very similar between the isotropic and anisotropic cases for the fundamental Lamb modes A_0 and S_0. However, this is no longer true for the SH_0 mode. Even though, for the value considered ($W_{400} = -4.0 \times 10^{-3}$), there are no caustics, the variations in group velocity around the 45° angle (and by symmetry around 135°) are strong enough to cause a perturbation that cannot simply be subtracted in order to highlight the effects of stress alone. The coupling of the two effects is not simply additive.

These initial results are essential for achieving our objective of characterising the stresses through the application of a more advanced inversion, as they demonstrate that the complex interaction between lamination and the effects of stresses on wave propagation can be decoupled from the effects of texture (by subtraction), at least for the two fundamental Lamb modes. Consequently, it should be straightforward to use these modes in an inversion process similar to that implemented in our previous study with an isotropic natural state.

3.2 Parametric studies for various frequencies

The results presented in this subsection generalise those obtained in the previous one by examining how

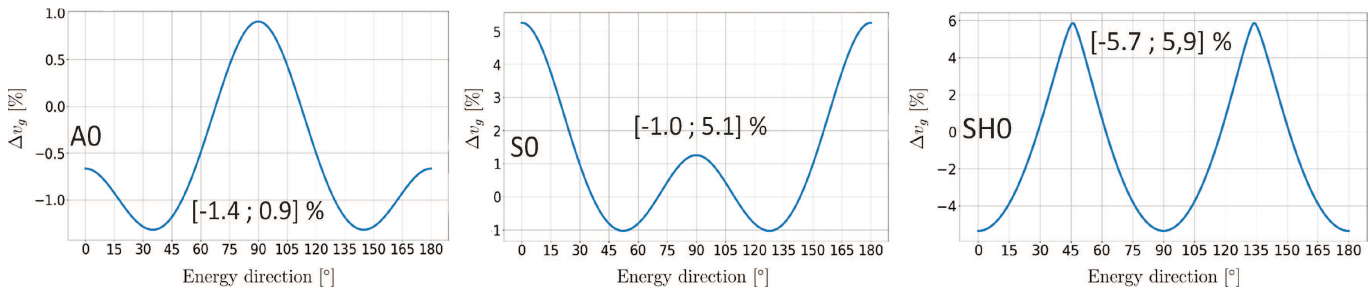

Figure 7. Anisotropy induced due to rolling ($W_{400} = -4 \times 10^{-3}$). The variations in terms of group velocity are estimated relatively to the isotropic plate before rolling.

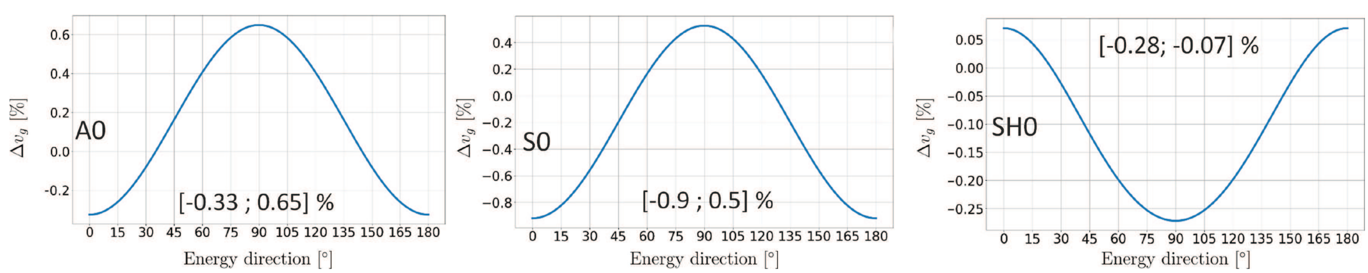

Figure 8. Anisotropy induced by a stressed state ($\sigma_1 = 500\,\mathrm{MPa}$). The variations in terms of group velocity are estimated relatively to the isotropic, unconstrained plate.

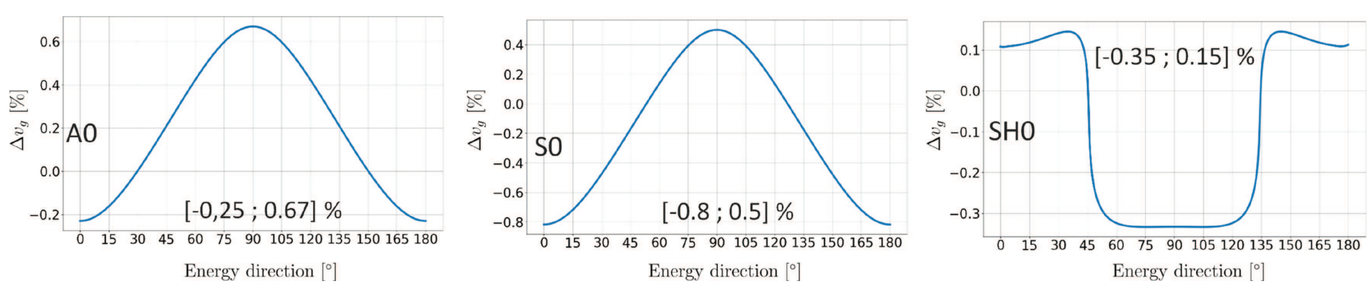

Figure 9. Variations in terms of group velocity for a stressed rolled plate ($\sigma_1 = 500\,\mathrm{MPa}$) relatively to the anisotropic unstressed rolled plate.

energy velocity variations evolve as functions of the frequency. This is an important consideration, as the application of the tomographic reconstruction method involves time-of-flight measurements; this means that the excitation signal must have a certain bandwidth so that the time difference between the arrival of a given signal and that of a reference signal can be easily measured, which is impossible with continuous-wave excitation. Here, the S_0 mode is considered in a wide bandwidth below the first cut-off frequency. Four results are shown and fully described in the figure caption of Figure 10. Results were obtained for the same set of parameters as before. The result important here is that one shown on the right column for the bottom row. This is the frequency-dependent generalization of that shown on Figure 9. The combined effect of rolling and stress, after simple subtraction of rolling effect, are very similar to what is obtained for stress effect in an isotropic (unrolled) plate, whatever the frequency considered. Similar results were obtained for the A_0 mode. Therefore, the use of these two modes excited by a pulse having a certain bandwidth can be considered as it was done in our previous studies on plates with isotropic natural state.

3.3 Obtaining of invertible functions usable in tomography

As shown in the previous subsection, once the effects of natural anisotropic state have been simply subtracted from the results obtained for a rolled and stressed plate, the variations of energy velocity in all directions are almost the same as those obtained in our previous study [2], which considered an isotropic natural state. This is true for Lamb waves below the first cut-off frequency. This was also verified for the shear horizontal mode but only for low absolute value of W_{400}. Therefore, when such similar behaviour is observed, developing an inversion method in the present case of a (anisotropic) rolled plate can be done as it was done previously when the natural state is isotropic [1].

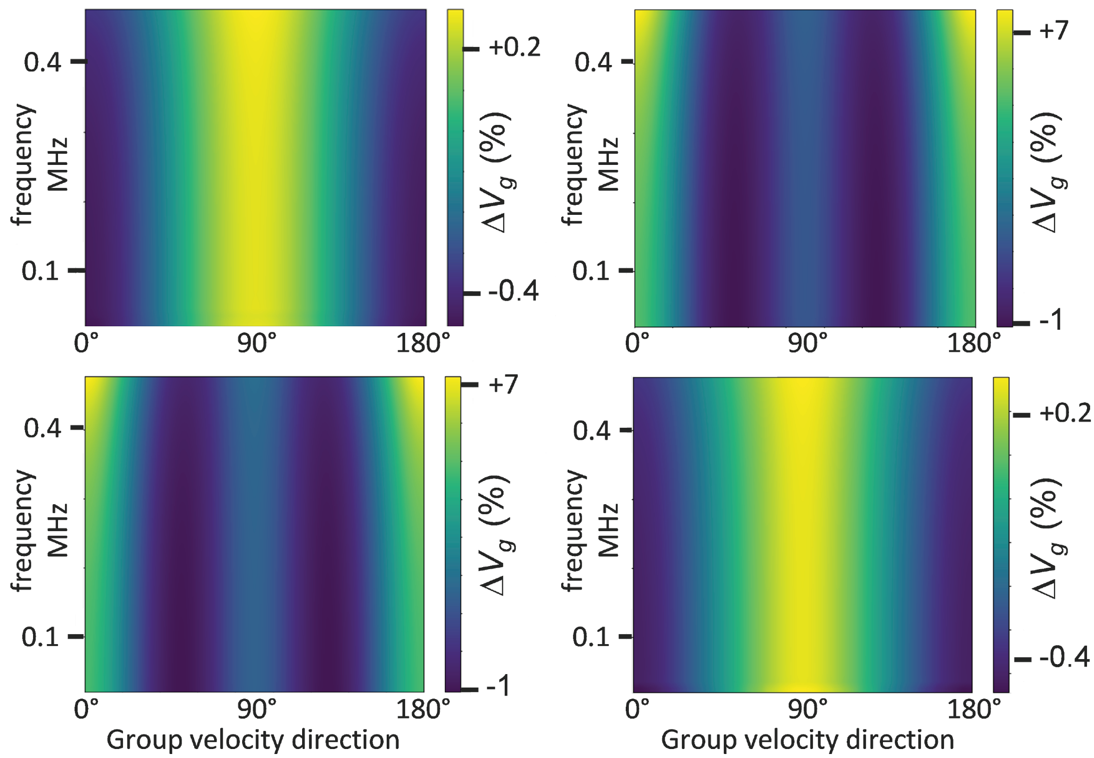

Figure 10. Variations of group velocities as functions of group velocity direction and of frequency. Top-left: variations induced by stress ($\sigma_1 = 500\,\text{MPa}$) relative to an isotropic natural state. Bottom-left: variations induced by rolling ($W_{400} = -4 \times 10^{-3}$) relative to isotropic natural state. Top-right: variations induced by stress ($\sigma_1 = 500\,\text{MPa}$) and rolling ($W_{400} = -4 \times 10^{-3}$) relative to an isotropic natural state. Bottom-right column: simple subtraction Top-right – Bottom-left.

For this, it is necessary to describe the variations of energy velocity with the energy velocity direction as simple functions that are invertible. Following our previous study, it can be seen that a typical approximation of these variations Δv^M can be written as follows if one considers that the directions 1 (rolling) and 2 are the principal direction of stress:

$$\Delta v^M = A^M(f)(\sigma_1 + \sigma_2) + B^M(f)\cos(2\beta)(\sigma_1 - \sigma_2) \quad (6)$$

where σ_1 and σ_2 are the in-plane stresses, β is the direction of energy velocity, and where $A^M(f)$ and $B^M(f)$ are two coefficients dependent on frequency specific to the mode M considered. Figure 11 shows how a simulated variation of energy velocity with direction is approximated by such a function. The curve is that for the A_0 mode at 100 kHz in the same rolled plate as before that is subjected to a stress σ_1 of 500 MPa. The function that fits the simulated results is simple as it only implies the prior determination of two frequency-dependent coefficients; it leads to simple inversion of wavespeed variation measurements.

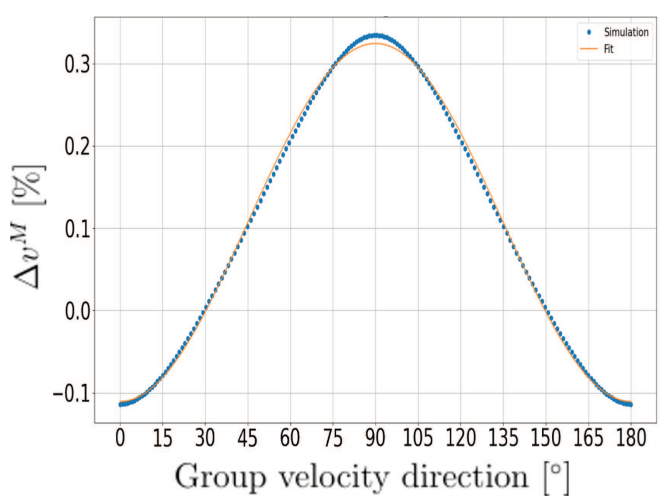

Figure 11. Example of fit of energy velocity variations with a simple invertible function as given by equation (6). Here, the A_0 mode is considered in the same rolled and stressed plate as the one considered in the previous subsection.

Next results in Figure 12 show how the coefficients $A^M(f)$ and $B^M(f)$ vary with frequency. They are given for the two fundamental Lamb modes. On each figure, the coefficients in solid lines (resp., in dashed lines) are predicted for a plate of isotropic (resp., transversely isotropic) natural state.

The frequency dependence of each coefficient is specific to the mode under consideration. Regardless of the symmetry of the natural modes, the variations follow similar patterns. However, they must be accurately determined to ensure precise inversions, as they clearly depend on the sheet's intrinsic anisotropy. This shows that

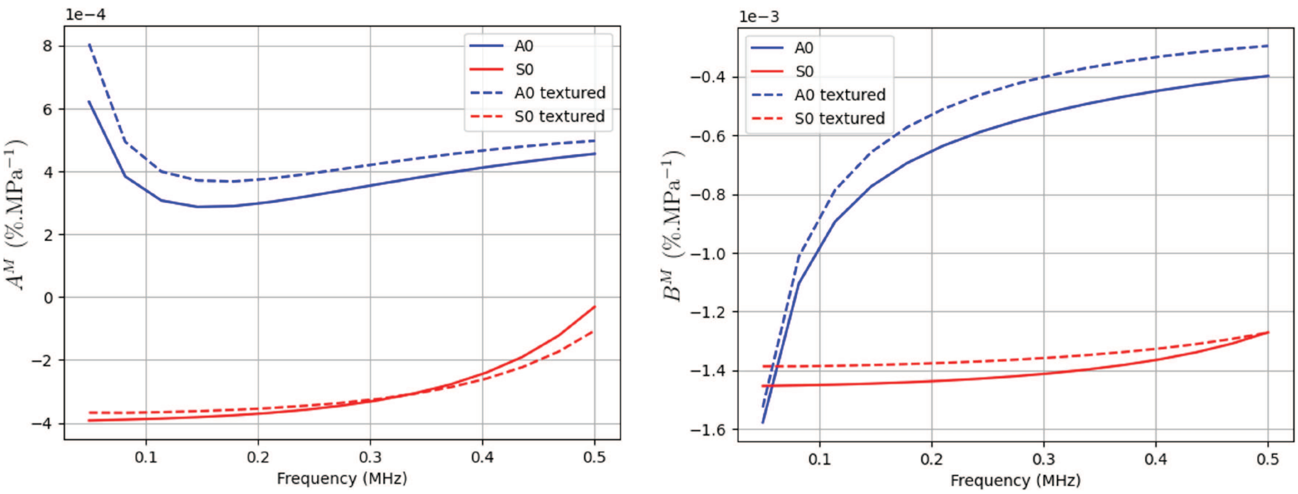

Figure 12. Variation of acoustoelastic coefficients used in equation (6) (left: coefficient A^M, right: coefficient B^M). Comparison of stressed plate vs. isotropic and stressed and textured vs. textured only.

(i) the effects of lamination (structuring) and stress do not simply add together, but combine in a complex manner, yet (ii) subtracting the effect of lamination from the combination of the two effects is sufficient to characterise the stresses through the acoustoelastic effect they have on guided waves.

Once this has been demonstrated, it becomes possible to go further and to use these invertible fitted functions in a tomographic inversion algorithm as this has been successfully done in [1].

4 Conclusion

In this study, we have developed a theoretical model capable of predicting the propagation of guided waves in plates subjected to both multiaxial stresses and initial anisotropy induced by rolling, by extending a recent model in which only stresses were taken into account [1]. It combines a semi-analytical finite element method (AE-SAFE) with simplified descriptions of texture and acoustoelasticity. It has been validated by comparing its predictions with those calculated using a time-domain finite element code.

Extensive parametric studies have shown that the combined effects of rolling and stresses on guided wave velocity can be effectively separated in certain cases of interest. For the fundamental Lamb modes (A_0 and S_0), the initial anisotropy due to rolling can be subtracted from the global velocity variations. However, the correct use of these Lamb modes for tomographic inversion requires the prior determination of acoustoelastic coefficients, which depend on the natural state anisotropy.

Conversely, the horizontal shear mode (SH_0) requires greater caution, particularly in cases of high anisotropy associated with strong rolling. For this mode, the formation of caustics makes it impossible or imprecise to measure a single velocity within a specific range of propagation directions. This means that these angular ranges must be systematically excluded from the tomographic inversion process.

These results have therefore made it possible to determine when and how the tomographic inversion method – initially developed for isotropic natural states – can be applied to mapping non-uniform distributions of residual stresses in rolled sheets.

Overall, these theoretical and numerical results pave the way for a more reliable and non-destructive characterisation of residual stresses in an industrial setting. Future work will focus on the experimental validation of this methodology on rolled sheets subjected to controlled stresses, ultimately leading to the practical implementation of a tomographic method for stress reconstruction.

Acknowledgments

The authors would like to extend special thanks to **Alexandre IMPERIALE** for his support in conducting the numerical validations.

Funding

This work was supported in part by the Agence Nationale de la Recherche, France, through the Research Project-ENCORE- under Grant ANR-22-CE42-0029-01.

Conflicts of interest

The authors declare that they have no known competing financial interests or personal relationships that could have appeared to influence the work reported in this paper.

Data availability statement

Data are available on request from the authors.

Author contribution statement

Flavien AGON: Conceptualization, Methodology, Formal analysis, Software, Writing – original draft. **Alain LHÉMERY**: Conceptualization, Methodology, Software, Writing – Review & Editing. **Jordan BARRAS**: Software – Review & Editing.

References

1. A. Abderahmane, A. Lhémery, L. Daniel: Stress imaging by guided wave tomography based on analytical acoustoelastic model. The Journal of the Acoustical Society of America 151 (2022) 2863–2876.
2. A. Abderahmane, A. Lhémery, L. Daniel: The effect of multiaxial pre-stress on Lamb and shear horizontal guided waves. The Journal of the Acoustical Society of America 149 (2021) 1724–1736. Erratum – The Journal of the Acoustical Society of America 151 (2022) 3315.
3. B. Zhang, C. Othmani, T. Khelfa, H. Zhang, C. Lü, A. Njeh: Acoustoelastic guided and surface waves in waveguides with focus on non-destructive testing and structural health monitoring applications – A review of recent studies. International Journal of Non Linear Mechanics 167 (2024) 104912.
4. J. Barras, A. Lhémery: Modal pencil method for the radiation of guided wave fields in composite plates of finite size. NDT & E International 126 (2022) 102598.
5. A. Dalmora, A. Imperiale, S. Imperiale, P. Moireau: A time-domain spectral finite element method for acoustoelasticity: modeling the effect of mechanical loading on guided wave propagation. Wave Motion 129 (2024) 103328.
6. S.Y. Jo, S. Hong, H.N. Han, M. Lee: Modeling and simulation of steel rolling with microstructure evolution: an overview. Steel Research International 94 (2023) 2200260.
7. M. Hirao, H. Ogi: Online texture monitoring of steel sheets, in: Electromagnetic Acoustic Transducers – Noncontacting Ultrasonic Measurements Using EMAT. Springer Series in Measurement Science and Technology. Springer, Tokyo, 2017, pp. 219–231.
8. K. Kawashima: Nondestructive characterization of texture and plastic strain ratio of metal sheets with electromagnetic acoustic transducers. The Journal of the Acoustical Society of America 87, 2 (1990) 681–690.

Cite this article as: Agon F. Lhémery A. & Barras J. 2026. From the simulation of guided wave propagation in rolled plates subjected to stress to the tomographic reconstruction of stress distributions. Acta Acustica, **10**, 61. https://doi.org/10.1051/aacus/2026058.